Electromagnetic Particle-in-Cell Simulations of Electron Holes Formed During the Electron Two-Stream Instability

2013 Plasma Sci. Technol. 15 17

(http://iopscience.iop.org/1009-0630/15/1/04)

Electromagnetic Particle-in-Cell Simulations of Electron Holes Formed During the Electron Two-Stream Instability*

WU Mingyu (吴明雨), LU Quanming (陆全明), ZHU Jie (朱洁),
WANG Peiran (王沛然), WANG Shui (王水)

CAS Key Lab of Geospace Environment, Department of Geophysics and Planetary Science, University of Science and Technology of China, Hefei 230026, China

Abstract Previous electrostatic particle-in-cell (PIC) simulations have pointed out that electron phase-space holes (electron holes) can be formed during the nonlinear evolution of the electron two-stream instability. The parallel cuts of the parallel and perpendicular electric field have bipolar and unipolar structures in these electron holes, respectively. In this study, two-dimensional (2D) electromagnetic PIC simulations are performed in the $x-y$ plane to investigate the evolution of the electron two-stream instability, with the emphasis on the magnetic structures associated with these electron holes in different plasma conditions. In the simulations, the background magnetic field ($\mathbf{B}_{\rm o} = B_{\rm o}\vec{e_x}$) is along the x direction. In weakly magnetized plasma ($\Omega_{\rm e} < \omega_{\rm pe}$, where $\Omega_{\rm e}$ and $\omega_{\rm pe}$ are the electron gyrofrequency and electron plasma frequency, respectively), several 2D electron holes are formed. In these 2D electron holes, the parallel cut of the fluctuating magnetic field δB_x and δB_z has unipolar structures, while the fluctuating magnetic field δB_y has bipolar structures. In strongly magnetized plasma ($\Omega_{\rm e} > \omega_{\rm pe}$), several quasi-1D electron holes are formed. The electrostatic whistler waves with streaked structures of E_y are excited. The fluctuating magnetic field δB_x and δB_z also have streaked structures. The fluctuating magnetic field δB_x and δB_y are produced by the current in the z direction due to the electric field drift of the trapped electrons, while the fluctuating magnetic field δB_z can be explained by the Lorentz transformation of a moving quasielectrostatic structure. The influences of the initial temperature anisotropy on the magnetic structures of the electron holes are also analyzed. The electromagnetic whistler waves are found to be excited in weakly magnetized plasma. However, they do not have any significant effects on the electrostatic structures of the electron holes.

Keywords: electron two-stream instability, particle-in-cell simulation

PACS: *52.35.Qz, 52.65.Rr*

DOI: 10.1088/1009-0630/15/1/04

1 Introduction

Electron phase-space holes (electron holes) have often been detected in different regions of the Earth's magnetosphere [1~7] and the solar wind [8]. In electron holes, the parallel cut of the electric field parallel to the ambient magnetic field has bipolar structures, while the signals of the electric field perpendicular to the ambient magnetic field are unipolar [2,3]. Electron holes are stationary Bernstein-Greene-Kruskal (BGK) solutions of the Vlasov-Poisson equations [9~12] and considered to be related to nonlinear Landau damping [13]. Electron holes have also been observed in laboratory experiments, for example, in a magnetized plasma surrounded by a waveguide [14], an unmagnetized laser-generated plasma [15] and during the magnetic reconnection experiments in a laboratory [16].

It has been known that counter-streaming electron beams can generate the electron two-stream instability, and electron holes can be formed during its nonlinear evolution [17]. One-dimensional (1D) particle-in-cell (PIC) simulations have shown that electron holes produced during the nonlinear evolution of the electron two-stream instability have positive electrostatic potentials, and therefore the parallel cut of the parallel electric field has a bipolar structure. These electron holes can remain stable for thousands of electron plasma periods [18~21]. Two-dimensional (2D) electrostatic PIC simulations have also been performed to study the nonlinear evolution of the electron two-stream instability, and the electrostatic structures of the formed electron holes are also investigated thoroughly [22~25]. The structures of electron holes are found to be governed by the combined actions between the transverse instability and the stabilization by the background magnetic field [25]. The transverse instability is a self-focusing type of instability. Perturbations in electron holes can produce transverse gradients of the electric potential. Such transverse gradients focus the trapped electrons into regions that already have a surplus of electrons,

*supported by Ocean Public Welfare Scientific Research Project, State Oceanic Administration People's Republic of China (No. 201005017), National Natural Science Foundation of China (Nos. 41274144, 41174124, 40931053, 41121003), CAS Key Research Program KZZD-EW-01, 973 Program (2012CB825602), and the Fundamental Research Funds for the Central Universities (WK2080000010)

which results in larger transverse gradients and more focusing until the transverse instability finally occurs [26]. In weakly magnetized plasma ($\Omega_e < \omega_{pe}$, where Ω_e and ω_{pe} are the electron gyrofrequency and electron plasma frequency, respectively), the electron holes formed during the electron two-stream instability have 2D structures (isolated along both the parallel and perpendicular directions). In these electron holes, the parallel cut of the perpendicular electric field ($E_\perp$) has unipolar structures, while the parallel cut of the parallel electric field ($E_\parallel$) has bipolar structures. In strongly magnetized plasma ($\Omega_e > \omega_{pe}$), the formed electron holes during the electron two-stream instability have quasi-1D structures, where a series of islands (with alternately positive and negative $E_\perp$) are developed along the direction perpendicular to the background magnetic field. The unipolar structures of the perpendicular electric field ($E_\perp$), as well as the bipolar structures of the parallel electric field ($E_\parallel$), are also formed in these electron holes. Such structures of electron holes have also been observed by the Polar and Fast Auroral Snapshot (FAST) satellites [2~4]. At the same time, the electrostatic whistler waves may be excited in strongly magnetized plasma and destroy the unipolar structures of the perpendicular electric field ($E_\perp$) associated with the electron holes. The electron temperature anisotropy can also affect the stabilization of electron holes. In a weakly magnetized plasma system, the increase of the electron perpendicular thermal velocity tends to stabilize the electron hole [27].

Although the electrostatic structures of the electron holes formed during the nonlinear stage of the electron two-stream instability have been thoroughly studied [23,25], recent observations found that there exist regular magnetic field signatures associated with the electron holes [28]. In this paper, we present 2D electromagnetic PIC simulations to further study the magnetic structures associated with electron holes formed during the nonlinear evolution of the electron two-stream instability under different plasma conditions.

This paper is organized as follows. In section 2, we described the simulation model. The simulation results are presented in section 3. Finally, the discussion and conclusions are given in section 4.

2 Simulation model

A 2D electromagnetic PIC code with periodic boundary conditions is employed in our simulations. This code has already been used to study the particle dynamics in magnetic reconnection [29]. The simulation system is taken in the $x-y$ plane with a uniform magnetic field $\mathbf{B}_0$ along the x direction. In this code ions are assumed to be infinitely massive and their dynamics are excluded. Essentially we consider two electron beam components. The initial velocity distributions of the two electron components are both bi-Maxwellian. Initially, these two electron components have the same density ($n_{e1} = n_{e2} = 0.5n_0$), the same parallel and perpendicular temperatures ($T_{||e1} = T_{||e2} = T_{||e}$, $T_{\perp e1} = T_{\perp e2} = T_{\perp e}$, where $T_{||e}$ and $T_{\perp e}$ are the parallel and perpendicular temperatures, respectively). The drift velocities of these two electron components are equal in magnitude but opposite in direction, and their drift velocities are V_b and $-V_b$, respectively.

In the simulations, the dimensionless units used have the density in the total unperturbed density n_0 ($n_0 = n_{e1} + n_{e2}$), the velocity in the electron parallel thermal velocity $v_{T_{||e}} = \sqrt{T_{||e}/m_e}$. We normalized space by the Debye length $\lambda_D = (\varepsilon_0 T_{||e}/n_0 e^2)^{1/2}$, and time by the inverse of the electron plasma frequency $\omega_{pe} = (n_0 e^2/m_e\varepsilon_0)^{1/2}$. The electric field is expressed in unit of $m_e\omega_{pe}v_{T_{||e}}/e$ and the magnetic field is expressed in unit of $m_e\omega_{pe}/e$. In addition, current densities are normalized by $\varepsilon_0 m_e\omega_{pe}^2 v_{T_{||e}}/e$, the potential by $T_{||e}/e$, and the energy by $n_0 T_{||e}/\varepsilon_0$.

Grid size units $\lambda_D \times \lambda_D$ are used in the simulations, and the time step is $0.02\omega_{pe}^{-1}$. There are 400 particles for each electron component in every cell, and the number of cells used in the simulations is 256×256. In our model, we choose the light speed as $c/v_{T_{||e}} = 20.0$, and $V_b = 2.0v_{T_{||e}}$.

3 Simulation results

In this paper, our main interest is focused on the electromagnetic signatures associated with the electron holes formed during the nonlinear evolution of the electron two-stream instability under different plasma conditions. A total of 4 runs are performed and the key parameters are given in Table 1. The parameters are similar with previous electrostatic PIC simulations, where we can observe obvious electron holes formed during the nonlinear evolution of the electron two-stream instability [25]. Runs 1 and 2 investigate the influences of the background magnetic field, and Runs 3 and 4 consider the effects of the initial electron temperature anisotropy. In the following part, we firstly show the results of Run 1, and then discuss these effects separately.

Table 1. Summary of simulations (Runs 1~4)

Run number	Ω_e	$v_{\|e}$	$v_{\perp e}$
1	0.6	1	1
2	2	1	1
3	0.6	1	5
4	2	1	5

Fig. 1 shows the overall evolution of the electric field energies E_x^2, E_y^2 and the fluctuating magnetic field energy $\delta B^2 = \delta B_x^2 + \delta B_y^2 + \delta B_z^2$ for Run 1. Here, Run 1 corresponds to weakly magnetized plasma. At about $\omega_{pe}t = 20$, with the excitation of the two-stream instability, the electric field energy E_x^2 begins to grow rapidly. When the electric field energy E_x^2 is sufficiently

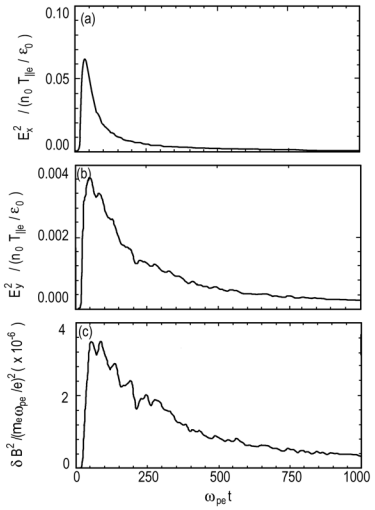

Fig.1 The time evolution of the electric field energies (a) E_x^2, (b) E_y^2, and (c) the fluctuating magnetic field energy $\delta B^2 = \delta B_x^2 + \delta B_y^2 + \delta B_z^2$ for Run 1. The electric field energies are normalized by $n_0 T_{||e}/\varepsilon_0$, and the magnetic field energies are normalized by $(m_e\omega_{pe}/e)^2$

large, nonlinear kinetic effects develop and parts of particles are trapped by the waves. The electric field energy E_y^2 and the fluctuating magnetic field energy δB^2 begin to increase. At about $\omega_{pe}t$ =40, E_x^2 reaches its maximum value, while the electric field energy E_y^2 and the fluctuating magnetic field energy δB^2 attain their maximum values a little later.

The evolution of the electromagnetic field for Run 1 is shown in Fig. 2, which plots (a) E_x, (b) E_y, (c) δB_x, (d) δB_y, and (e) δB_z at $\omega_{pe}t$ =40, 400, and 820, respectively. With the excitation of the two-stream instability, monochromatic waves are firstly excited and have a substantial degree of coherence perpendicular to the background magnetic field, as described at the time $\omega_{pe}t$ =40. After the saturation of the two-stream instability, the nonlinear dynamic behaviors dominate the evolution. These monochromatic waves begin to merge with each other at the point with the closest approach between two waves. Finally, several 2D electron holes, which are isolated in both the parallel and perpendicular directions, are formed, and their parallel cut of E_x has bipolar structures. These 2D electron holes are the results of combined actions between the transverse instability and stabilization by the background magnetic field, and they may have a positive or negative propagation speed along the background magnetic field, or almost stay stationary. As time goes on, such 2D electron holes become weaker and weaker. At the time $\omega_{pe}t$ =820, some electron holes are too weak to be observed.

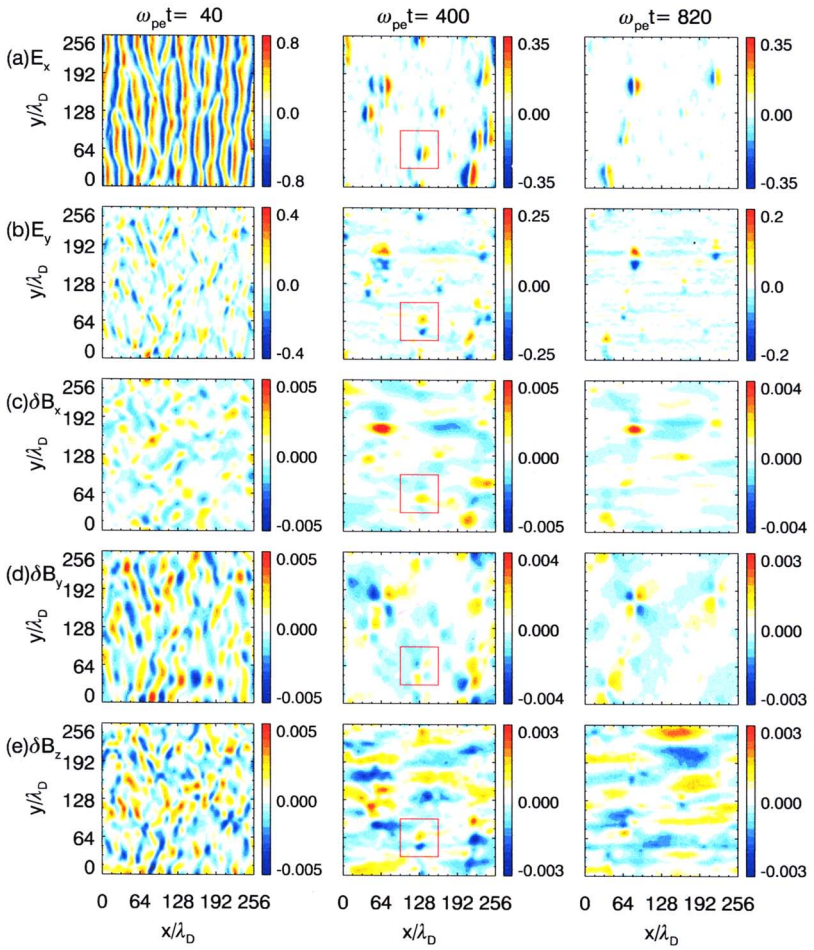

Fig.2 Panels (a)∼(e) display the electric field components (a) E_x, (b) E_y, and the fluctuating magnetic field components (c) δB_x, (d) δB_y, (e) δB_z at $\omega_{pe}t$ =40, 400 and 820 for Run 1 (color online)

In order to analyze the electromagnetic signatures of the electron holes in detail, we select the electron hole in $96\lambda_{\rm D} < x < 160\lambda_{\rm D}$ and $32\lambda_{\rm D} < y < 96\lambda_{\rm D}$ at $\omega_{\rm pe}t$ =400 (the region encircled by red line in Fig. 2). Obviously, the parallel cut of E_y is observed to have unipolar structures, which is consistent with the results in 2D electrostatic PIC simulations [25]. Such unipolar structures have also been obtained in previous theoretical works on multi-dimensional BGK modes [30,31]. At the same time, the fluctuating magnetic fields associated with the electron hole also have regular structures. δB_x has unipolar structures and the value of δB_x is always positive in the electron hole. δB_y has quadrupole structures, whose parallel cut is bipolar. The parallel cut of δB_z has unipolar structures, while the value of δB_z is positive in the upper part of the electron hole and negative in the lower part. The formation of the fluctuating magnetic fields δB_x and δB_y in an electron hole can be described as follows: due to the existence of the perpendicular electric field E_y, the trapped electrons in the electron hole will suffer the electric field drift along the z direction, which can be expressed as $v_{Ez} \approx -E_y/B_0$. Therefore, the current along the z direction is formed in the electron hole (Ions, which cannot be trapped in the electron hole with positive potential, may also suffer electric field drift in the electron hole. However, their drift motions are too complicated to be described by a simple expression because their gyroradii are larger than the spatial scales of the electron hole and their effects on the current along the z direction are negligible.), which then generates the fluctuating magnetic field δB_x and δB_y associated with the electron hole. In these electron holes, the value of j_z is positive in the upper part and negative in the lower part. Therefore, the fluctuating magnetic field δB_x is enhanced in the center of the 2D electron hole with positive values, while δB_y has quadruple structures. The structures of the fluctuating magnetic field δB_y can be interpreted based on the Lorentz transformation of a moving quasi-electrostatic structure [28]. The fluctuating magnetic field δB_z can be described as

$$\delta B_z = \frac{v_{\rm EH}}{c^2} E_y, \qquad (1)$$

where $v_{\rm EH}$ is the propagation speed of the electron hole, which is parallel to the background magnetic field $\mathbf{B}_0$. Therefore, a propagating electron hole will generate the fluctuating magnetic field δB_z with the same structures as E_y, whose parallel cut has unipolar structures. In this Run, the propagation speed of the selected electron hole is about $v_{\rm EH} = 1.0 v_{T_{||\rm e}}$, and δB_z is estimated to be about $0.0025 E_y$ based on Eq. (1), which is consistent with our simulation results.

3.1 The effects of the background magnetic field

Figs. 3 and 4 describe the simulation results for Run 2, which corresponds to strongly magnetized plasma. Fig. 3 shows the overall evolution of the electric field energies E_x^2, E_y^2 and the fluctuating magnetic field energy $\delta B^2 = \delta B_x^2 + \delta B_y^2 + \delta B_z^2$, while Fig. 4 plots (a) E_x, (b) E_y, (c) δB_x, (d) δB_y and (e) δB_z at $\omega_{\rm pe}t$ = 40, 460, and 760, respectively. Compared with weakly magnetized plasma, now the evolution of the electric field energy and the fluctuating magnetic field energy becomes slower due to the strong stabilization effects on the transverse instability by the background magnetic field. We can also find that both E_y^2 and δB^2 increase at about $\omega_{\rm pe}t$ =300 due to the excitation of electrostatic whistler waves. At the same time, the formed electron holes in strongly magnetized plasma have quasi-1D structures (the extension along the y direction is infinite), and they can persist for a sufficiently long time without breaking into segments until the end of the simulation. In these quasi-1D electron holes, the bipolar structures of E_y are firstly formed, as shown at $\omega_{\rm pe}t$ =460, and then the the bipolar structures evolve into the unipolar structures. A series of islands (with alternately positive and negative E_y) develop in the electron holes along the direction perpendicular to the background magnetic field, which can last for about several hundreds of plasma periods. Therefore, in strongly magnetized plasma, we can also observe the bipolar and unipolar structures for the parallel cut of E_x and E_y, respectively, which are the same as in weakly magnetized plasma. However, the electron holes are unstable to the electrostatic whistler waves in strongly magnetized plasma. The electrostatic whistler waves are a generalization of Langmuir waves and often observed in the multi-dimensional PIC simulations of electron two-stream instability [22~25]. The electrostatic whistler waves begin to be excited at about

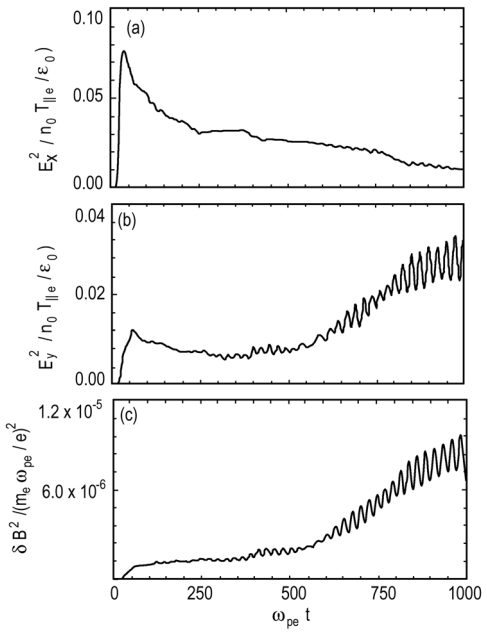

Fig.3 The time evolution of the electric field energies (a) E_x^2, (b) E_y^2, and (c) the fluctuating magnetic field energy $\delta B^2 = \delta B_x^2 + \delta B_y^2 + \delta B_z^2$ for Run 2. The electric field energies are normalized by $n_0 T_{||\rm e}/\varepsilon_0$, and the magnetic field energies are normalized by $(m_{\rm e}\omega_{\rm pe}/e)^2$

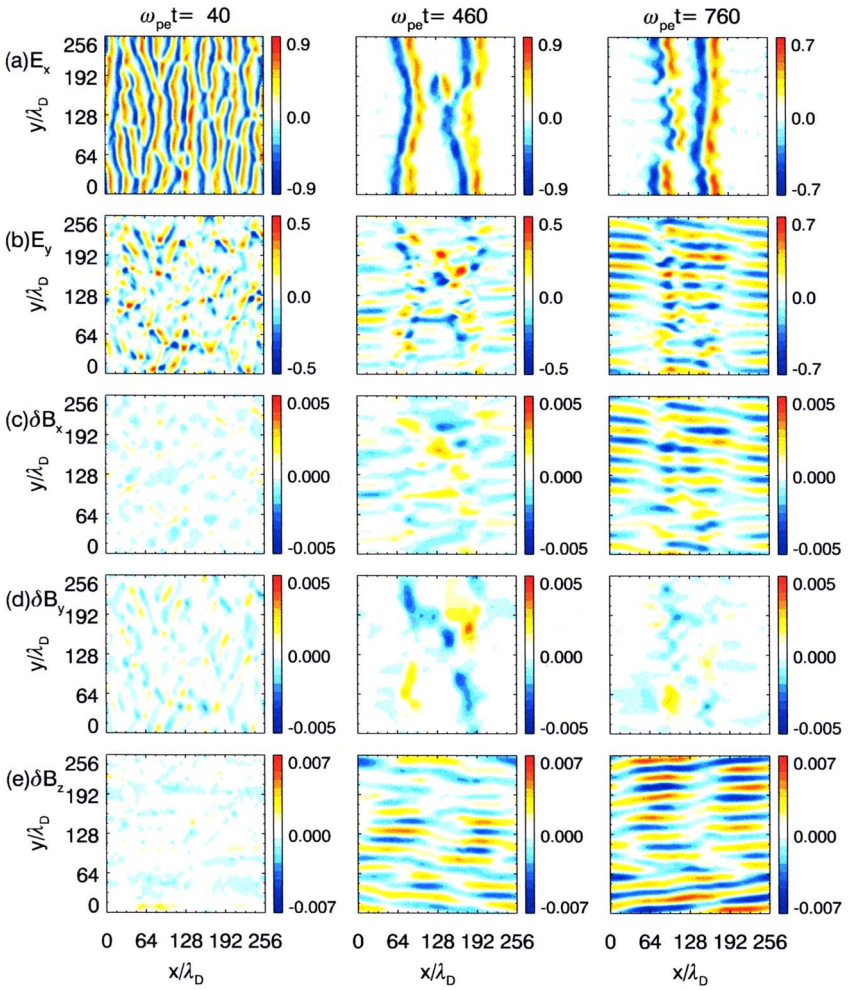

Fig.4 Panels (a)∼(e) display the electric field components (a) E_x, (b) E_y, and the fluctuating magnetic field components (c) δB_x, (d) δB_y, (e) δB_z at $\omega_{\rm pe}t$ =40, 460 and 760 for Run 2 (color online)

$\omega_{\rm pe}t = 500$. As proposed by WU et al. [24], the generation mechanisms of the electrostatic whistler waves can be described as follows: at first, the perpendicular electric field E_y in electron holes can influence the electron trajectories which pass through the electron holes, which leads to the variation of the charge density along the y direction outside of the electron holes, and the streaked structures of E_y are formed. Then, the interactions between the streaked structures of E_y outside the electron holes and the vibration of the kinked electron holes emit the electrostatic whistler waves. The current j_z is generated by the electron electric field drift motions along the z direction due to the existence of E_y. The current j_z produces the fluctuating magnetic field δB_x and δB_y. Because of the streaked structures of the current j_z, the amplitude of δB_y is much smaller than that of δB_x. The generation mechanism of the fluctuating magnetic field δB_z is due to the propagation of the electrostatic whistler waves along the x direction. According to Eq. (1), we can know that the propagating electrostatic whistler waves can produce the streaked structures of the fluctuating magnetic field δB_z, as shown in the Fig. 4. The electrostatic whistler waves will at last destroy the unipolar structures of E_y.

3.2 The effects of the initial electron temperature anisotropy

Runs 3 and 4 analyze the effects of initial electron temperature anisotropy on the evolution of electron two-stream instability for weakly and strongly magnetized plasma conditions, respectively. Fig. 5 shows the overall evolution of the electric field energies E_x^2, E_y^2 and the fluctuating magnetic field energy $\delta B^2 = \delta B_x^2 + \delta B_y^2 + \delta B_z^2$ for Run 3. Fig. 6 plots (a) E_x and (b) E_y at the time $\omega_{\rm pe}t = 40$, 400, and 820, while Fig. 7 plots (a) E_z, (b) δB_x, (c) δB_y and (d) δB_z at the same time as Fig. 6 for Run 3. Before about $\omega_{\rm pe}t = 50$ (which is indicated by the dash lines in Fig. 5), the time evolution of two-stream instability is the same as that of Run 1. At about $\omega_{\rm pe}t = 50$, the electromagnetic whistler modes begin to be excited. The amplitude of electromagnetic whistler modes reaches the maximum around $\omega_{\rm pe}t = 290$ and then decays. The electromagnetic whistler waves are right-hand wave mode and propagate along the ambient magnetic field, which are excited by the electron temperature anisotropy [32∼34]. The generations of electromagnetic whistler modes have been previously investigated by both theoretic

studies and particle simulations. LU et al. used one-dimensional PIC simulations to investigate the electromagnetic instabilities generated by the electron temperature anisotropy in a homogenous plasma system [34]. They found that the electromagnetic whistler modes are excited and the dispersion relations are consistent with the cold plasma theory. In Run 3, the structures of δB_y and δB_z at $\omega_{\rm pe}t = 400$ are consistent with the prediction of the one-dimensional simulations.

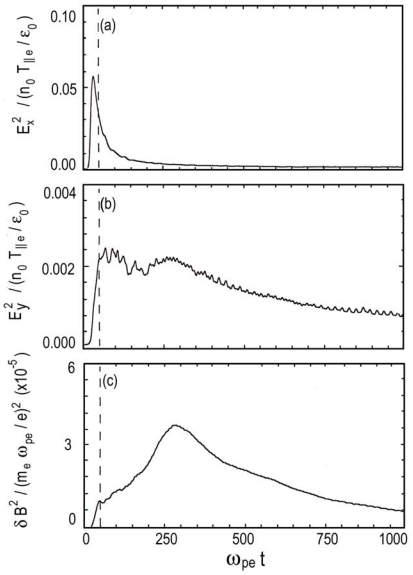

Fig.5 The time evolution of the electric field energies (a) E_x^2, (b) E_y^2, and (c) the fluctuating magnetic field energy $\delta B^2 = \delta B_x^2 + \delta B_y^2 + \delta B_z^2$ for Run 3. The electric field energies are normalized by $n_0 T_{||e}/\varepsilon_0$, and the magnetic field energies are normalized by $(m_e\omega_{\rm pe}/e)^2$

Therefore, two types of instabilities are excited in this Run. One is the electrostatic electron two-stream instability, and the other is the electromagnetic whistler waves. The electric fields E_x and E_y are dominated by the electrostatic electron two-stream instability. E_x and E_y have bipolar and unipolar structures in the electron holes, respectively, and their evolutions are slower than that in Run 1 due to the stabilization of the electron temperature anisotropy. E_z and the fluctuating magnetic field components δB_y and δB_z are dominated by the electromagnetic whistler waves. The fluctuating magnetic field δB_x can also been affected by the electromagnetic whistler waves, and its amplitude is much smaller than that of δB_y and δB_z in this Run.

Fig. 8 plots (a) E_x, (b) E_y, (c) δB_x, (d) δB_y and (e) δB_z at $\omega_{\rm pe}t = 40$, 460, and 760 for Run 4. The results of this run are similar to those of Run 2. And in this Run, the electromagnetic whistler waves cannot be excited.

4 Discussion and conclusion

The magnetic structures of 2D electron holes have already been investigated by DU et al. [35] with 2D electromagnetic PIC simulation in weakly magnetized plasma. In their simulations, an initial 1D electron hole is assumed to exist in the simulation domain. The 1D electron hole is broken into several 2D electron holes, and the magnetic structures associated with these electron holes have regular structures. In this paper, we have performed 2D electromagnetic PIC simulations to study the structures of the fluctuating magnetic field associated with electron holes formed during the nonlinear evolution of the electron two-stream instability. In weakly magnetized plasma, several 2D electron holes are formed. In these 2D electron holes, in addition to the bipolar structures of the parallel electric field E_x, there still exists the unipolar structures of the perpendicular electric field E_y due to the transverse instability. In strongly magnetized plasma, the electrostatic waves dominate the evolution of the fluctuating magnetic field. In such a plasma system, both δB_x and δB_y have streaked structures while δB_y is too weak to be observed. The generation mechanism of the fluctuating magnetic field is the same as in DU et al [35]. The fluctuating magnetic field δB_x and δB_y are produced by the current in the z direction due to the electric field drift of the electrons. The fluctuating magnetic field δB_z can be explained by the Lorentz transforming of a moving quasi-electrostatic structure. We further found that in weakly magnetized plasma, the electromagnetic whistler waves are unstable to the electron temperature anisotropy. However, they have little influence on the electrostatic structures of the electron holes.

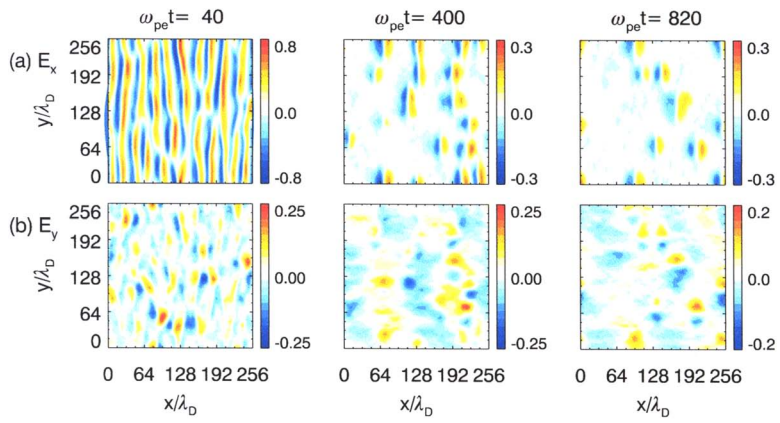

Fig.6 Panels (a)∼(b) display the electric field components (a) E_x and (b) E_y at $\omega_{\rm pe}t = 40$, 400 and 820 for Run 3 (color online)

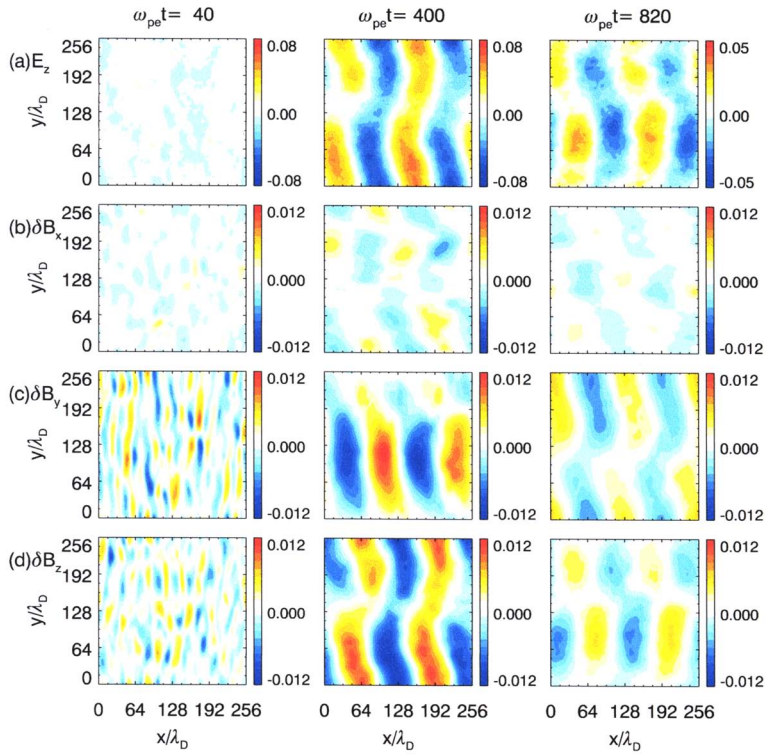

Fig.7 Panels (a)∼(d) display the electric field components (a) E_z and the fluctuating magnetic field components (b) δB_x, (c) δB_y, (d) δB_z at $\omega_{\rm pe}t = 40$, 400 and 820 for Run 3 (color online)

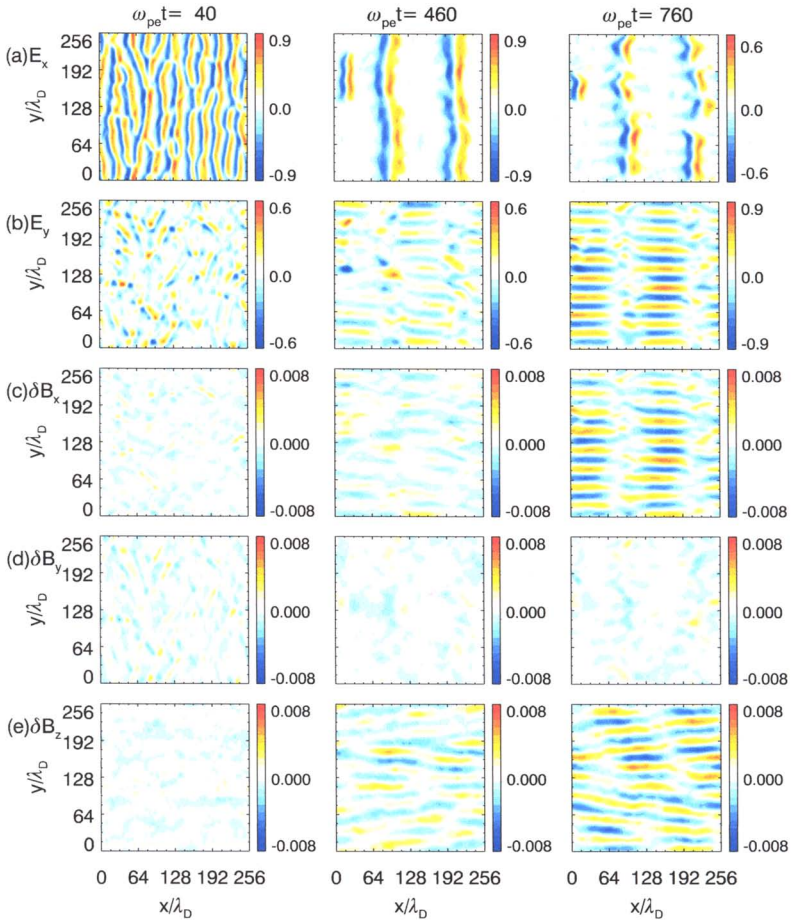

Fig.8 Panels (a)∼(e) display the electric field components (a) E_x, (b) E_y, and the fluctuating magnetic field components (c) δB_x, (d) δB_y, (e) δB_z at $\omega_{\rm pe}t = 40$, 460 and 760 for Run 4 (color online)

References

1 Matsumoto H, Kojima H, Miyatake T, et al. 1994, Geophys. Res. Lett., 21: 2915
2 Ergun R E, Carlson C W, McFadden J P, et al. 1998, Geophys. Res. Lett., 25: 2041
3 Ergun R E, Carlson C W, McFadden J P, et al. 1998, Phys. Rev. Lett., 81: 826
4 Franz J R, Kintner P M, and Pickett J S. 1998, Geophys. Res. Lett., 25: 1277
5 Pickett J S, Chen L J, Kahler S W, et al. 2004, Ann. Geophys., 22: 2515
6 Bale S D, Kellogg P J, Larson D E, et al. 1998, Geophys. Res. Lett., 25: 2929
7 Cattell C J, Crumley J, Dombeck J, et al. 2002, Geophys. Res. Lett., 29: 1065
8 Mangeney A, Salem C, Lacombe C, et al. 1999, Ann. Geophys., 17: 307
9 Bernstein I B, Greene J M, and Kruskal M D. 1957, Phys. Rev., 108: 546
10 Chen L J, Pickett J, Kintner P, et al. 2005, J. Geophys. Res., 110: A09211
11 Muschietti L, Ergun R E, Roth I, et al. 1999, Geophys. Res. Lett., 26: 1093
12 Ng C S and Bhattacharjee A. 2005, Phys. Rev. Lett., 95: 245004
13 Ng C S, Bhattacharjee A and Skiff F. 2006, Phys. Plasmas, 13: 055903
14 Saeki K, Michelsen P, Pecseli H L, et al. 1979, Phys. Rev. Lett., 42: 501
15 Sarri, Dieckmann M E, Brown C R D, et al. 2010, Phys. Plasmas, 17: 010701
16 Fox W, Porkolab M, Egedal J, et al. 2008, Phys. Rev. Lett., 101: 255003
17 Roberts K V, and Berks H L. 1967, Phys. Rev. Lett., 19: 297
18 Omura Y, Kojama H, and Matsumoto H. 1994, Geophys. Res. Lett., 21: 2923
19 Mottez F, Perraut S, Roux A, et al. 1997, J. Geophys. Res., 102: 11399
20 Lu Q M, Wang S, and Dou X K. 2005, Phys. Plasmas, 12: 072903
21 Lu Q M, Wang D Y and Wang S. 2005, J. Geophys. Res., 110: A03223
22 Goldman M V, Oppenheim M, and Newman D L. 1999, Geophys. Res. Lett., 26: 181
23 Oppenheim M, Newman D L, and Goldman M V. 1999, Phys. Rev. Lett., 83: 2344
24 Umeda T, Omura Y, Miyake T, et al. 2006, J. Geophys. Res., 111: A10206
25 Lu Q M, Lembege B, Tao J B, et al. 2008, J. Geophys. Res., 113: A11219
26 Muschietti L, Roth I, Carlson C W, et al. 2000, Phys. Rev. Lett., 85: 94
27 Wu M Y, Wu H, Lu Q M, et al. 2010, Chin. Phys. Lett., 27: 095201
28 Andersson L, Ergun R E, Tao J, et al. 2009, Phys. Rev. Lett., 102: 225004
29 Fu X R, Lu Q M and Wang S. 2006, Phys. Plasmas, 13: 012309
30 Chen L J and Parks G K. 2002, Geophys. Res. Lett., 29: 1331
31 Muschietti L, Roth I, Carlson C W, et al. 2002, Nonlin. Processes in Geophys., 9: 101
32 Gary S P and Cairns I H. 1999, J. Geophys. Res., 104: 19835
33 Gary S P and Wang J. 1996, J. Geophys. Res., 101: 10749
34 Lu Q M, Wang L Q, Zhou Y, et al. 2004, Chin. Phys. Lett., 21: 1518
35 Du A, Wu M Y, Lu Q M, et al. 2011, Phys. Plasmas, 18: 032104

(Manuscript received 3 August 2011)
(Manuscript accepted 8 November 2011)
E-mail address of corresponding author LU Quanming: qmlu@ustc.edu.cn